IEICE TRANSACTIONS

on Electronics

DOI:10.1587/transele.2023SEP0002

Publicized:2023/10/25

A PUBLICATION OF THE ELECTRONICS SOCIETY

The Institute of Electronics, Information and Communication Engineers

Kikai-Shinko-Kaikan Bldg., 5-8, Shibakoen 3chome, Minato-ku, TOKYO, 105-0011 JAPAN

Paper

Estimation of Core Size Distribution of Magnetic Nanoparticles using High-T_c SQUID Magnetometer and Particle Swarm Optimizer-based Inversion Technique

Mohd Mawardi Saari[†a)], ***Nonmember***, **Mohd Herwan Sulaiman**[††], ***Nonmember and*** **Toshihiko Kiwa**[†††], ***Member***

SUMMARY In this work, the core size estimation technique of magnetic nanoparticles (MNPs) using the static magnetization curve obtained from a high-T_c SQUID magnetometer and a metaheuristic inversion technique based on the Particle Swarm Optimizer (PSO) algorithm is presented. The high-T_c SQUID magnetometer is constructed from a high-T_c SQUID sensor coupled by a flux transformer to sense the modulated magnetization signal from a sample. The magnetization signal is modulated by the lateral vibration of the sample on top of a planar differential detection coil of the flux transformer. A pair of primary and excitation coils are utilized to apply an excitation field parallel to the sensitive axis of the detection coil. Using the high-T_c SQUID magnetometer, the magnetization curve of a commercial MNP sample (Resovist) was measured in a logarithmic scale of the excitation field. The PSO inverse technique is then applied to the magnetization curve to construct the magnetic moment distribution. A multimodal normalized log-normal distribution was used in the minimization of the objective function of the PSO inversion technique, and a modification of the PSO search region is proposed to improve the exploration and exploitation of the PSO particles. As a result, a good agreement on the Resovist magnetic core size was obtained between the proposed technique and the non-negative least square (NNLS) inversion technique. The estimated core sizes of 8.0484 nm and 20.3018 nm agreed well with the values reported in the literature using the commercial low-T_c SQUID magnetometer with the SVD and NNLS inversion techniques. Compared to the NNLS inversion technique, the PSO inversion technique had merits in exploring an optimal core size distribution freely without being regularized by a parameter and facilitating an easy peak position determination owing to the smoothness of the constructed distribution. The combination of the high-T_c SQUID magnetometer and the PSO-based reconstruction technique offers a powerful approach for characterizing the MNP core size distribution, and further improvements can be expected from the recent state-of-the-art optimization algorithm to optimize further the computation time and the best objective function value.

key words: *Magnetic nanoparticle, High-T_c SQUID, magnetometer, magnetization curve, and magnetic core size distribution.*

†The author is with Faculty of Electrical & Electronics Engineering Technology and Centre for Advanced Industrial Technology, Universiti Malaysia Pahang Al-Sultan Abdullah, Pahang 26600, Malaysia.
††The author is with Faculty of Electrical & Electronics Engineering Technology, Universiti Malaysia Pahang Al-Sultan Abdullah, Pahang 26600, Malaysia.
†††The author is with Graduate School of Interdisciplinary Science & Engineering in Health Systems, Okayama University, Okayama 700-8530, Japan.
a) Corresponding Author, E-mail: mmawardi@ump.edu.my

1. Introduction

Determination of the core size of magnetic nanoparticles (MNPs) is essential in tailoring their performances for specific applications such as magnetic particle imaging (MPI) [1], magnetic immunoassay [2], and magnetic hyperthermia [3]. For this purpose, the information regarding the core size can be measured directly by transmission electron microscopy (TEM) or indirectly using static magnetization measurement and X-ray diffraction (XRD) [4], [5]. Since the applications of MNPs are based on the magnetic properties upon application of external fields, the static magnetization measurement is commonly used to characterize the MNP core size distribution, although this indirect method requires solving an inverse problem of the MNP magnetization curve.

The static magnetization curve of MNPs can be measured using the vibrating sample magnetometer (VSM) using a normal induction coil where the induction coil senses the magnetization of an MNP sample upon application of a DC field. Improved measurement sensitivity can be obtained by using a magnetometer that is based on the low-T_c superconducting quantum interference device (SQUID), such as the commercial SQUID Magnetometer MPMS 3 (Quantum Design, USA). However, the usage of expensive liquid ^{4}He and complex thermal insulation configuration has resulted in a higher running cost for low-T_c SQUID magnetometers [6]. On the other hand, the application of the high-T_c superconductors discovered in early 1990 has been rapidly increasing such that the high-T_c SQUID is expected to play a major role in enabling highly sensitive applications owing to its low-running cost and simpler thermal insulation. It has been reported in [7] that the high-T_c SQUIDs showed a field noise of 25 fT/Hz$^{1/2}$ at 1 kHz and 77 K, comparable to the low-T_c SQUID. For an application that requires a high excitation field application to a sample, i.e., magnetization curve measurement, the flux transformer technique can be used to sense the magnetization of the sample [8]. Apart from that, the high-T_c SQUIDs have been used to perform magnetic nanoparticle-based molecular diagnostics [9], magnetic needle biopsy [10], and magnetic detection of magnetically

tagged biological cells [11]–[13].

Previous studies have demonstrated that the core size of MNPs can be reliably reconstructed using the magnetic moment distribution obtained from the static magnetization curve [14]–[16]. This core size is a critical parameter that predominantly determines the specific application of MNPs. Compared to the direct measurement of core size using transmission electron microscopy, estimating the core size from the MNP magnetization curve is relatively easy and faster. Typically, the core size of an MNP ensemble can be estimated by solving the inverse problem of its magnetization curve. The degree of MNP magnetization directly corresponds to the magnetization of individual MNP cores, where larger cores exhibit larger magnetic moments following the Langevin function. By solving the inverse problem, solutions are obtained, representing the distribution of magnetic moments, which can then be used to derive the core size. Various algorithms, such as singular value decomposition (SVD) [15], non-negative least squares (NNLS) [16], [17], and iterative Kaczmarz, have been proposed for this purpose [4]. However, these methods may require regularization and threshold determination techniques to address overfitting issues in ill-conditioned problems, which can lead to biased or inaccurate magnetic moment reconstruction. As an alternative, recent advancements in intelligent algorithms, particularly in machine learning and optimization areas, have offered promising solutions to engineering problems, and these machine learning algorithms can be utilized to solve the inverse problem of the MNP magnetization curve without the need for regularization.

In this study, we present a high-T_c SQUID magnetometer utilizing an induction coil as the flux transformer to characterize the magnetization curve of MNPs. Then, utilizing the magnetometer, we introduce a magnetization curve reconstruction technique based on a metaheuristic algorithm, namely, Particle Swarm Optimizer (PSO), to estimate the core size distribution of a commercial magnetic nanoparticle sample. By using PSO, we aim to obtain accurate and unbiased reconstructions of the magnetic moment distribution, thus enabling us to derive the core size distribution of the magnetic nanoparticles.

2. High T_c-SQUID Magnetometer and Reconstruction of Magnetization Curve

2.1 High T_c-SQUID Magnetometer for MNP Magnetization Curve Measurement

Figure 1 illustrates the schematic diagram of the custom-designed high-T_c SQUID magnetometer. The high-T_c SQUID was developed using an advanced multilayer fabrication technique by the Superconducting Sensing Technology Research Association (SUSTERA; formerly known as ISTEC), Japan [7], [8], [18]. The mutual inductance of the 59-turn superconducting input coil was determined to be 1.95 nH. This input coil is connected to a first-order planar differential coil. Each coil of the planar differential coil has 200 turns, 451.6 μH inductance, 2.99 Ω DC resistance, and the two coils are separated by a 13.5-mm baseline. To enhance the cancellation of high magnetic fields, a manually tuned compensation coil is integrated in series with the differential coil. The combined configuration of the planar gradiometer and the compensation coil achieves a remarkable cancellation factor of $B_{detected}/B_{applied}$ of 0.02%. During the magnetization curve measurement, different DC magnetic fields are applied to the sample consecutively. The resolution and range of the magnetization field are improved by using a pair of primary and secondary excitation coils, where the former enables the field excitation range up to 500 mT, and the latter improves the field resolution based on a difference feedback control. The magnetization signal from a sample is subsequently modulated by reciprocating it along the baseline of the planar differential coil at a frequency of 11.6 Hz, and the sample magnetization is captured using a lock-in amplifier at a time constant of 300 ms.

In this study, we investigated the core size distribution of multi-core Resovist (FUJIFILM RI Pharma, Japan), having a core size of 8.3 nm measured using a transmission electron microscopy (TEM) (TEM LIBRA 120, ZEISS) at 120 kV, and hydrodynamic size of 61 nm measured using a particle analyzer based on the dynamic light scattering (DLS) technique (Litesizer 500, Anton Paar GmbH, Austria). The iron concentration of MNPs was diluted to 0.26 mg/mL from the stock solution, and a 0.77 mL sample volume was used for the measurement. The MNP magnetization was measured from 0.5 to 500 mT on a logarithmic scale.

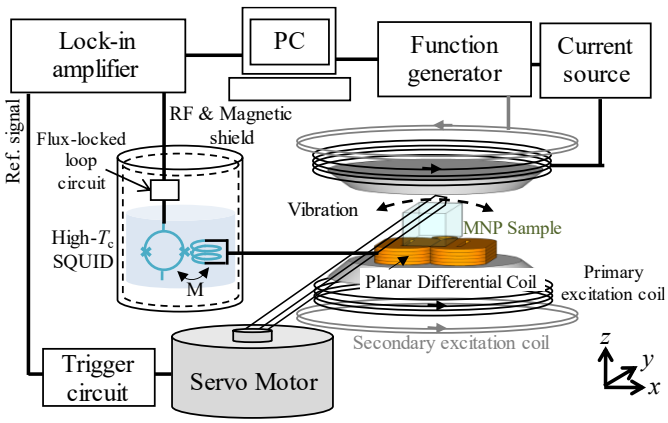

Fig. 1 High-T_c SQUID Magnetometer.

2.2 Reconstruction of Magnetization Curve using Particle Swarm Optimizer-based Inversion Technique

The magnetization M of a monodisperse magnetic nanoparticle ensemble subjected to a magnetization field $\mu_0 H$ can be described using the Langevin equation $L(m\mu_0 H/k_B T) = \mathrm{Coth}(m\mu_0 H/k_B T) - 1/(m\mu_0 H/k_B T)$ [14]:

$$M(\mu_0 H) = M_{sat} L(m\mu_0 H / k_B T), \quad (1)$$

where M_{sat} is the saturation magnetization, m is the magnetic moment, μ_0 is the vacuum magnetic permeability, H is the applied field intensity, k_B is the Boltzmann constant and T is the temperature. Moreover, the resulting MNP magnetization curve of a finite polydisperse core size distribution can be expressed by [19]:

$$\begin{aligned} M(\mu_0 H) &= \int n(m) m L(m\mu_0 H / k_B T) dm \\ &\approx \sum_{i=1}^{N} n_i m_i L(m_i \mu_0 H_j / k_B T) \Delta m_i \\ &\approx \sum_{i=1}^{N} w_i L(m_i \mu_0 H_j / k_B T) \ . \end{aligned} \quad (2)$$

Here, $w_i(m)$ represents the product of the number of particles n_i with a magnetic moment m_i within the range of m_i to $m_i+\Delta m_i$. Since the magnetization curve is formed by different point J of applied magnetic fields, Eq. (2) can be expressed in the vector form of $\mathbf{M}= \mathbf{L}\,\mathbf{w}$, where vectors $\mathbf{M}$, $\mathbf{L}$, and $\mathbf{w}$ can be represented by $M_j \equiv M(\mu_0 H_j)$ (j = 1,…, J), $L_{ji} = L(m_i \mu_0 H_j / k_B T)$ and $w_i(m) \equiv n_i(m) m_i \Delta m_i$ (i = 1,…, N), respectively.

The reconstruction of the distribution of $w_i(m)$, i.e., nm^2, from a measured magnetization curve $\mathbf{M}_{\exp}$ can be obtained by minimizing the mean squares deviation ξ^2:

$$\xi^2 = \left\| \mathbf{M}_{\exp} - \mathbf{L}\mathbf{w} \right\|^2 . \quad (3)$$

between the measured magnetization and magnetization model. This minimization process can be obtained through appropriate methods such as SVD, NNLS, and optimization algorithms such as PSO. The minimization process will produce the vector $\mathbf{w}$, which contains individual weights of their Langevin equation. Then, the core size of MNP having magnetic moment m can be derived by assuming a spherical shape core:

$$D_c = \sqrt[3]{\frac{6}{\pi} \frac{m}{M_{sat}}} \ . \quad (4)$$

Detailed explanations of SVD and NNLS methods for the magnetization curve reconstruction can be found in [15] and [16], respectively.

PSO is a metaheuristic optimization algorithm inspired by the social behavior of swarm animals, such as birds flocking. Briefly, PSO starts with a group of particles representing potential solutions to an optimization problem. Each particle adjusts its position based on its current velocity, personal best position, and the best position found by any particle in the swarm. By iteratively updating positions and velocities, particles explore the search space, aiming to converge toward the optimal solution. The algorithm continues until a termination condition is met, making PSO a preferable method for approximating solutions to various optimization problems [20], [21]. The solution obtained from PSO is based on the exploration and exploitation processes of the particles, and it should be noted that the solution might be trapped in local minima instead of global optima, resulting in a poor agreement between the reconstructed and measured magnetization curves [22]. Moreover, the constructed core size distribution may produce spikes and noises that do not physically resemble the actual core size distribution. To improve the core size estimation using PSO, $w(m)$ is assumed to have a multimodal normalized log-normal distribution, i.e., summation of K modal distributions, and is expressed by

$$w(m) = \sum_{k=1}^{K} g_k \exp\left(\frac{\ln m - \ln \mu_{m,k}}{2\sigma_{m,k}^2}\right) , \quad (5)$$

where g_k, $\sigma_{m,k}$ and $\mu_{m,k}$ are the distribution weight, standard deviation, and mean of k^{th} m-distribution, respectively.

In the PSO inversion technique, the optimal values of g_k, $\sigma_{m,k,}$ and $\mu_{m,k}$ are determined to minimize the objective function of Eq. (3). Each optimal value is searched within a search region set by the lower and upper bounds. In the conventional approach of using PSO, the lower and upper bounds can be set to include the entire region of possible solutions. However, in this study, we propose a modification of the PSO search region for $\mu_{m,k}$ to improve the exploration and exploitation of the PSO particles. This modification will facilitate a non-overlapping search region of $\mu_{m,k}$ so that an optimal value of $\mu_{m,k}$ will be specific and unique to only the selected search region. This modification is implemented by separating the upper and lower bounds for each $\mu_{m,k}$ search region into k regions where $\mu_{m,k-1} < \mu_{m,k}$, as illustrated in Figure 2. In addition, separating the $\mu_{m,k}$ search region will also help the PSO algorithm to produce a global solution with improved precision.

On the other hand, the search region of $\sigma_{m,k,}$ is set from 0.5 to 1 so that the narrowest distribution will have a width of around one decade (logarithmic scale) while the widest distribution will have a width of around two decades, as shown in Table 1. g_k is set from 0 to 1, representing the distribution ratio of a M_s-normalized magnetization curve. It was observed that $\sigma_{m,k,}$ less than 0.5 would result in a sharp distribution spike/shape, which may not be physically correct. The PSO and NNLS inversion techniques are implemented using MATLAB on a Windows 10 AMD Ryzen 7 4700U 2 GHz 16 GB RAM. The PSO algorithm is based on the MATLAB Toolbox function, and a detailed explanation of PSO can be found in [23].

Table 1 Parameters of PSO Inversion Technique.

Parameter	Value/Range
Magnetic moment m	20 moments/decade
K	3
g_k	[0, 1]
$\sigma_{m,k}$	[0.5, 1]
$\mu_{m,k}$	$[10^{-21}, 10^{-16}]$ Am^2
PSO Maximum Iteration	1000
PSO Function Tolerance	1×10^{-9}
Swarm size	30

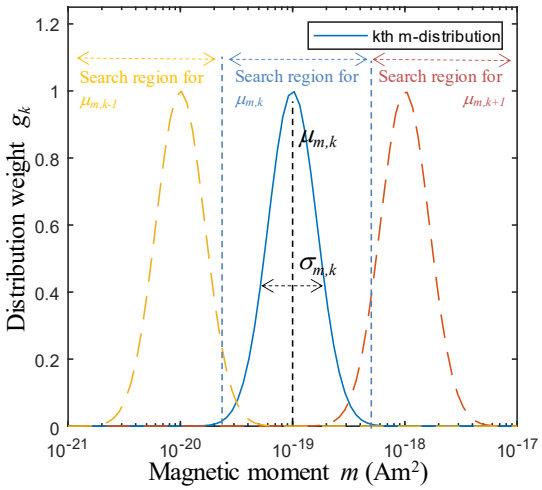

Fig. 2 Normalized log-normal distribution and its parameter search region.

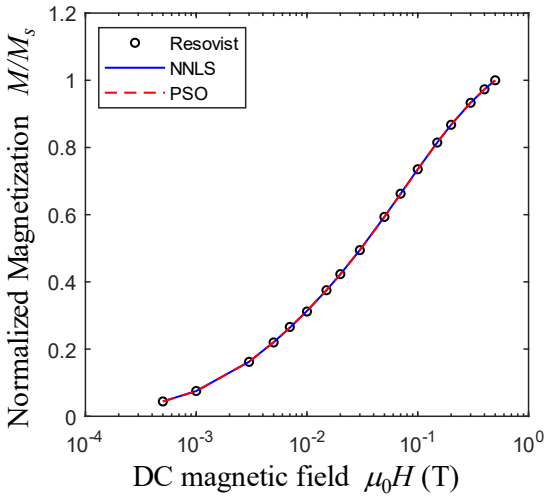

Fig. 3 Magnetization curves of the Resovist sample and its reconstructed curves using NNLS and PSO inversion techniques.

3. Results and Discussions

Figure 3 shows the magnetization curve of the Resovist sample measured using the high-T_c SQUID magnetometer between 0.5 to 500 mT. 17 measurement points of the sample magnetization were recorded on a logarithmic scale. The magnetization increased in a nonlinear manner with the applied field, reflecting the Langevin equation characteristic. The reconstructed magnetization curve using the PSO inversion technique is shown by the dashed red line in Figure 3. For comparison, the NNLS inversion technique was also applied and is shown by the blue line in Figure 3. It could be said that both inversion techniques had resulted in a good agreement with the measured magnetization data, and their best objective function, i.e., the mean squares deviation ξ^2, was fairly similar, as shown in Table 2. The convergence curve of PSO is shown in Figure 4, where the history of the objective function value with respect to the iteration number of PSO can be observed. It could be observed that the objective function was rapidly improved in the first 200 iterations, reflecting the effectiveness of the exploration process of the particles. The PSO inversion technique took 62.3 s for 1000 iterations to arrive at the best objective function value of 8.6805×10^{-6} in the total search region of 220 magnetic moments, as shown in Table 2. For comparison, the NNLS inversion technique was relatively fast (49.8 ms) in solving the inverse problem for the total search region of 120 magnetic moments. It is worth noting that the computation time of NNLS was improved because its iteration was separated into 10 subdomains, and 12 domains were evaluated in each iteration. The values of domain and subdomain acted as a regularization parameter where they affected the distribution shape of w, despite improving the calculation time. The domain and subdomain values were optimized priorly using the trial and error method to obtain a closed distribution shape with fewer spikes/noises [16], [24], [25].

The constructed w distributions with respect to m using the NNLS and PSO inversion techniques are shown in Figure 5. The w distribution from the PSO inversion technique was fundamentally constructed from the three m-distributions, shown by the yellow, cyan, and magenta lines in Figure 5, and their optimal g_k, $\sigma_{m,k}$ and $\mu_{m,k}$ values are tabulated in Table 2. From Table 2 and Figure 5, it could be said that only two dominant m-distributions existed in the Resovist sample and agreed well with the bimodal distribution form obtained from the NNLS inversion technique. Moreover, the peak positions for both inversion techniques were fairly similar, reflecting the ability of the PSO inversion technique to estimate the dominant peaks even though the trimodal distribution was assumed initially. Moreover, the w distribution from the PSO inversion technique was smoother than the NNLS inversion technique, facilitating an easy peak position determination.

From the m values of the peak positions, the core size of the Resovist sample was estimated using Eq. (4) and the saturation magnetization M_s=300 kA/m [19]. The core sizes determined from the PSO and NNLS inversion techniques are listed in Table 2, where both techniques reflected a fairly similar core size. The highest peak from the PSO inversion technique resulted in a core size of 8.0484 nm, while the second peak reflected a core size of 20.3018 nm. The elemental 8.0448 nm core size agreed with the TEM results, and the 20.3018 nm core size was inferred due to the aggregation on these elemental cores. The aggregation of the elemental cores would produce an effective magnetic core with higher m than the elemental core. Furthermore, these core sizes estimated in this work agreed well with the Resovist core sizes determined in [19], [26] in which the commercial low-T_c SQUID magnetometer with the SVD and NNLS inversion techniques had been used. Moreover, the reported core size of Resovist in the literature ranges from 5 to 10 nm for the elemental cores, and 20 to 26 nm for

the aggregated elemental core [19], [26]–[28] and the 0.3-nm difference of the elemental core size between the PSO and NNLS inversion technique would be acceptable when these size ranges were considered. When compared with the size determined from the TEM images (8.3 nm), the NNLS inversion technique (8.3647 nm) gave a closer value of the elemental core size. It was worth noting that the NNLS inversion technique showed the third (smallest) peak located at m=2.37×10^{-17} Am^2, which corresponded to a core size of 53.2235 nm. This core size for the Resovist sample had not been reported in the literature; however, the possibility of a small percentage of a bigger elemental core aggregation could not be completely ignored. Moreover, the existence of this peak in the NNLS inversion technique could be caused by the separation of domains and subdomains in the NNLS iteration, where the combined solution from all iterations could produce spikes/noises, as observed in [16], [24], [25].

Although the NNLS inversion technique showed a better computational time and objective function value, the PSO inversion technique had merit in terms of the shape smoothness of the constructed distribution and the ability to explore freely possible distribution numbers and width within expected search regions without being regularized by a parameter. It is worth noting that improvement in machine-learning techniques, such as PSO, has rapidly occurred in recent years, where some recent algorithms have been reported to outperform PSO in terms of computation time and objective function [22], [29]–[33]. This improvement can be achieved by inventing and implementing a robust and advanced method in the exploration and exploitation processes of an optimization algorithm, as shown in [29]. In the foreseeable future, we anticipate the emergence of a more advanced metaheuristic algorithm compared to PSO, which can be employed to address the MNP core size estimation problem. This advancement holds the promise of yielding improved results in terms of the objective function value, computation time and generating less biased reconstruction for intricate MNP magnetization curves.

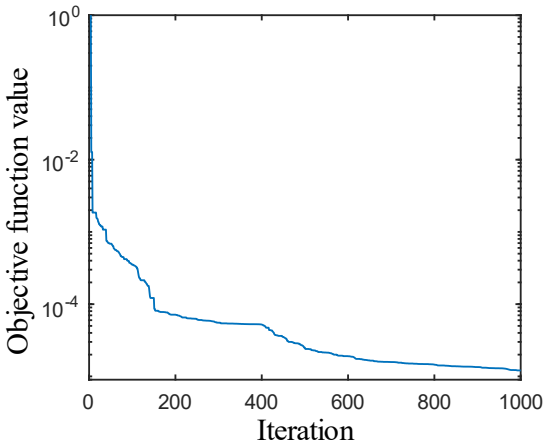

Fig. 4 Convergence curve of the PSO objective function (Eq. (3)). The best function value was 1.2084×10$^{-5,}$ and the computation time took 62.2781 s.

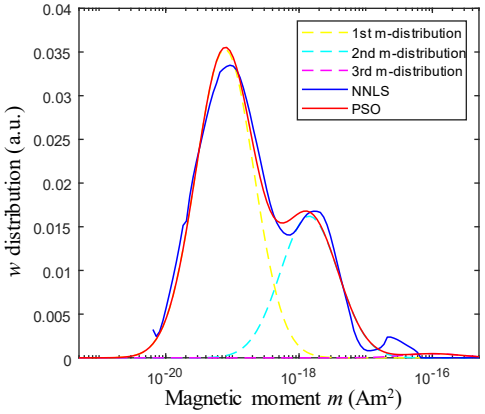

Fig. 5 Constructed weight w distribution of the Langevin function with respect to m using the NNLS and PSO inversion techniques. For PSO, the summation of 3 modal distributions (K=3), illustrated by 1st to 3rd m-distributions, was estimated.

Table 2 Results of PSO & NNLS Inversion Techniques.

Parameter	Value
g_1	0.0353
$\sigma_{m,1}$	1.0000
$\mu_{m,1}$	7.7163×10^{-20} Am^2
g_2	0.016207411
$\sigma_{m,2}$	0.9954
$\mu_{m,2}$	1.4210×10^{-18} Am^2
g_3	4.7296×10^{-4}
$\sigma_{m,3}$	0.9998
$\mu_{m,3}$	1.0000×10^{-16} Am^2
PSO Best Objective Function	1.2084×10^{-5}
PSO Computational Time	62.2781 s
NNLS Best Objective Function	8.6805×10^{-6}
NNLS Computational Time	0.0498 s
1st PSO Peak Core Size	8.0484 nm
2nd PSO Peak Core Size	20.3018 nm
1st NNLS Peak Core Size	8.3647 nm
2nd NNLS Peak Core Size	21.9290 nm

4. Conclusion

In this work, we determined the magnetic core size of the Resovist sample using the developed high-T_c SQUID magnetometer and the metaheuristic inversion technique based on the PSO algorithm. The high-T_c SQUID magnetometer demonstrated a sufficiently high sensitivity to resolve the magnetization curve of the MNP sample at a sub-milligram iron concentration. The proposed PSO inversion technique solved the nonlinear characteristic of the magnetization curve to derive the distribution of magnetic moment, i.e., core size. The estimated core sizes agreed well with the NNLS inversion technique and the sizes reported in the literature using the commercial low-T_c SQUID. This work demonstrated that the combination of the high-T_c SQUID magnetometer and the PSO-based reconstruction technique offers a powerful approach for characterizing and understanding the core size distribution of MNPs, which may contribute to the improvement of the MNP core size for

various applications in fields such as biomedicine, nanotechnology, and materials science. The MATLAB code for the PSO inversion technique is available at https://www.researchgate.net/publication/372494851_PSO_MH.

Acknowledgments

This work was supported by the Research Management Center of Universiti Malaysia Pahang under the International Publication Grant RDU223315.

References

[1] B. Gleich and J. Weizenecker, "Tomographic imaging using the nonlinear response of magnetic particles," *Nature*, vol. 435, no. 7046, pp. 1214–7, Jun. 2005, doi: 10.1038/nature03808.

[2] K. Kishimoto *et al.*, "Dispersion of Fe3O4Nanoparticle Beads Driven by Femtosecond Laser Pulses for Quantitative Magnetic Immunoassay Measurements," *ACS Appl. Nano Mater.*, 2022, doi: 10.1021/acsanm.2c04399.

[3] H. Chen *et al.*, "Tuning the dynamics in Fe3O4nanoparticles for hyperthermia optimization," *Appl. Phys. Lett.*, vol. 117, no. 7, 2020, doi: 10.1063/5.0017903.

[4] D. Schmidt, D. Eberbeck, U. Steinhoff, and F. Wiekhorst, "Finding the magnetic size distribution of magnetic nanoparticles from magnetization measurements via the iterative Kaczmarz algorithm," *J. Magn. Magn. Mater.*, 2016, doi: 10.1016/j.jmmm.2016.09.108.

[5] M. Mawardi Saari *et al.*, "Properties of single- and multi-core magnetic nanoparticles assessed by magnetic susceptibility measurements," *J. Magn. Magn. Mater.*, vol. 528, no. October 2020, p. 167812, 2021, doi: 10.1016/j.jmmm.2021.167812.

[6] K. Tsukada, K. Morita, Y. Matsunaga, M. M. Saari, K. Sakai, and T. Kiwa, "Hybrid Type HTS-SQUID Magnetometer With Vibrating and Rotating Sample," *IEEE Trans. Appl. Supercond.*, vol. 26, no. 3, pp. 1–5, Apr. 2016, doi: 10.1109/TASC.2016.2531632.

[7] S. Adachi, A. Tsukamoto, Y. Oshikubo, T. Hato, and K. Tanabe, "Fabrication of integrated HTS-SQUID magnetometers having multiturn input coils with different sizes," *Phys. C Supercond. its Appl.*, vol. 471, no. 21–22, pp. 1258–1262, Nov. 2011, doi: 10.1016/j.physc.2011.05.173.

[8] A. Tsukamoto, S. Adachi, Y. Oshikubo, K. Tanabe, and K. Enpuku, "Development of a HTS SQUID module for use with an external pickup coil," *Supercond. Sci. Technol.*, vol. 26, no. 1, p. 15013, Jan. 2013, doi: 10.1088/0953-2048/26/1/015013.

[9] M. I. Faley *et al.*, "High- T c SQUID biomagnetometers," *Supercond. Sci. Technol.*, vol. 30, no. 8, p. 083001, Aug. 2017, doi: 10.1088/1361-6668/aa73ad.

[10] H. C. Bryant *et al.*, "Magnetic Properties of Nanoparticles Useful for SQUID Relaxometry in Biomedical Applications.," *J. Magn. Magn. Mater.*, vol. 323, no. 6, pp. 767–774, Mar. 2011, doi: 10.1016/j.jmmm.2010.10.042.

[11] K. Yamashita *et al.*, "Aggregation of Magnetic Nanoparticles in Biological Solvents Evaluated by HTS-SQUID Magnetic Immunoassay System," *IEEE Trans. Appl. Supercond.*, vol. 33, no. 5, pp. 1–5, 2023, doi: 10.1109/TASC.2023.3239830.

[12] K. Enpuku *et al.*, "Characterization of Magnetic Markers for Liquid-Phase Immunoassays Using Brownian Relaxation," *Jpn. J. Appl. Phys.*, vol. 51, p. 023002, Jan. 2012, doi: 10.1143/JJAP.51.023002.

[13] A. Tsukamoto *et al.*, "Development of Multisample Biological Immunoassay System Using HTS SQUID and Magnetic Nanoparticles," *IEEE Trans. Appl. Supercond.*, vol. 15, no. 2, pp. 656–659, Jun. 2005, doi: 10.1109/TASC.2005.849988.

[14] M. M. Saari, K. Sakai, T. Kiwa, T. Sasayama, T. Yoshida, and K. Tsukada, "Characterization of the magnetic moment distribution in low-concentration solutions of iron oxide nanoparticles by a high- T c superconducting quantum interference device magnetometer," *J. Appl. Phys.*, vol. 117, no. 17, p. 17B321, May 2015, doi: 10.1063/1.4919043.

[15] D. V Berkov *et al.*, "New method for the determination of the particle magnetic moment distribution in a ferrofluid," *J. Phys. D. Appl. Phys.*, vol. 33, no. 4, pp. 331–337, Feb. 2000, doi: 10.1088/0022-3727/33/4/303.

[16] J. van Rijssel, B. W. M. Kuipers, and B. H. Erné, "Non-regularized inversion method from light scattering applied to ferrofluid magnetization curves for magnetic size distribution analysis," *J. Magn. Magn. Mater.*, vol. 353, pp. 110–115, Mar. 2014, doi: 10.1016/j.jmmm.2013.10.025.

[17] M. D. Woodhams and M. D. Hendy, "Reconstructing phylogeny by Quadratically Approximated Maximum Likelihood," *Bioinformatics*, vol. 20, no. suppl_1, pp. i348–i354, Aug. 2004, doi: 10.1093/bioinformatics/bth926.

[18] S. Adachi *et al.*, "Preparation of multilayer films for integrated high-Tc SQUIDs with ramp-edge Josephson junctions," *Phys. C Supercond.*, vol. 468, no. 15–20, pp. 1936–1941, Sep. 2008, doi: 10.1016/j.physc.2008.05.171.

[19] A. L. Elrefai, T. Yoshida, and K. Enpuku, "Magnetic parameters evaluation of magnetic nanoparticles for use in biomedical applications," *J. Magn. Magn. Mater.*, vol. 474, no. September 2018, pp. 522–527, 2019, doi: 10.1016/j.jmmm.2018.11.022.

[20] A. G. Gad, *Particle Swarm Optimization Algorithm and Its Applications: A Systematic Review*, vol. 29, no. 5. Springer Netherlands, 2022.

[21] E. H. Houssein, A. G. Gad, K. Hussain, and P. N. Suganthan, "Major Advances in Particle Swarm Optimization: Theory, Analysis, and Application," *Swarm Evol. Comput.*, vol. 63, no. March 2020, p. 100868, 2021, doi: 10.1016/j.swevo.2021.100868.

[22] M. H. Sulaiman, Z. Mustaffa, M. M. Saari, and H. Daniyal, "Barnacles Mating Optimizer: A new bio-inspired algorithm for solving engineering optimization problems," *Eng. Appl. Artif. Intell.*, vol. 87, no. October 2019, p. 103330, 2020, doi: 10.1016/j.engappai.2019.103330.

[23] J. Kennedy and R. Eberhart, "Particle swarm optimization," in *Proceedings of ICNN'95 - International Conference on Neural Networks*, 1995, vol. 4, pp. 1942–1948, doi: 10.1109/ICNN.1995.488968.

[24] J. Van Rijssel, B. W. M. Kuipers, and B. H. Erné, "Bimodal distribution of the magnetic dipole moment in nanoparticles with a monomodal distribution of the physical size," *J. Magn. Magn. Mater.*, vol. 380, pp. 325–329, 2015, doi: 10.1016/j.jmmm.2014.09.058.

[25] Y. Sun, N. Ye, D. Wang, Z. Du, S. Bai, and T. Yoshida, "An improved method for estimating core size distributions of magnetic nanoparticles via magnetization harmonics," *Nanomaterials*, vol. 10, no. 9, pp. 1–12, 2020, doi: 10.3390/nano10091623.

[26] K. Enpuku *et al.*, "Estimation of the effective magnetic anisotropy constant of multi-core based magnetic nanoparticles from the temperature dependence of the coercive field," *J. Appl. Phys.*, vol. 127, no. 13, 2020, doi: 10.1063/1.5144713.

[27] D. X. Chen, N. Sun, and H. C. Gu, "Size analysis of carboxydextran coated superparamagnetic iron oxide particles used as contrast agents of magnetic resonance imaging," *J. Appl. Phys.*, vol. 106, no. 6, 2009, doi: 10.1063/1.3211307.

[28] D. Eberbeck, F. Wiekhorst, S. Wagner, and L. Trahms, "How the size distribution of magnetic nanoparticles determines their magnetic particle imaging performance," *Appl. Phys. Lett.*, vol. 98, no. 18, p. 182502, 2011, doi: 10.1063/1.3586776.

[29] Z. Ma, G. Wu, P. N. Suganthan, A. Song, and Q. Luo, "Performance assessment and exhaustive listing of 500+ nature-inspired metaheuristic algorithms," *Swarm Evol. Comput.*, vol. 77, no. January, p. 101248, 2023, doi: 10.1016/j.swevo.2023.101248.

[30] L. Liu, C. Guo, Y. Tu, H. Mei, and L. Wang, "Differential Evolution

Fitting-Based Optical Step-Phase Thermography for Micrometer Thickness Measurement of Atmospheric Corrosion Layer," *IEEE Trans. Ind. Informatics*, vol. 16, no. 8, pp. 5213–5222, 2020, doi: 10.1109/TII.2019.2955493.

[31] R. Storn and K. Price, "Differential Evolution - A Simple and Efficient Heuristic for Global Optimization over Continuous Spaces," *J. Glob. Optim.*, vol. 11, no. 4, pp. 341–359, 1997, doi: 10.1023/A:1008202821328.

[32] H. Rakhshani and A. Rahati, "Snap-drift cuckoo search: A novel cuckoo search optimization algorithm," *Appl. Soft Comput. J.*, vol. 52, pp. 771–794, 2017, doi: 10.1016/j.asoc.2016.09.048.

[33] G. Zhang and Y. Shi, "Hybrid Sampling Evolution Strategy for Solving Single Objective Bound Constrained Problems," *2018 IEEE Congr. Evol. Comput. CEC 2018 - Proc.*, pp. 1–7, 2018, doi: 10.1109/CEC.2018.8477908.

Mohd Mawardi Saari received the B. E., M. E., and Ph.D. degrees from Okayama University, Okayama, Japan, in 2011, 2013, and 2015, respectively. He currently serves as an Associate Professor at the Faculty of Electrical & Electronics Engineering Technology, Universiti Malaysia Pahang (UMP). His research interest includes magnetometers for the evaluation of magnetic nanoparticles and non-destructive tests for defect evaluation in metal components.

Mohd Herwan Sulaiman obtained his B. Eng. (Hons) in Electrical-Electronics, M. Eng. (Electrical-Power), and Ph.D. (Electrical Engineering) from Universiti Teknologi Malaysia (UTM) in 2002, 2007, and 2012, respectively. He currently serves as an Associate Professor at the Faculty of Electrical & Electronics Engineering Technology, Universiti Malaysia Pahang (UMP). His research interests are power system optimization and swarm intelligence applications to power system studies. He is also a Senior Member of IEEE.

Toshihiko Kiwa received the B. E., M. E., and Ph.D. degrees from Osaka University in 1998, 2000, and 2003, respectively. After that, he worked for one year as a JSPS fellow at the Research Center for Superconductor Photonics, Osaka University, where he was involved in developing terahertz and superconductor devices. Currently, he is a professor at the Graduate School of Interdisciplinary Science and Engineering in Health Systems, Okayama University. His research interests include chemical sensors, magnetometric sensors, and terahertz sensing devices and systems.